


Article

Atomic Network-Based DOA Estimation Using Low-Bit ADC

Shuran Sheng^{1,2} , Peng Chen^{1,2,*} , Yuxuan Yao^{2,3}, Lenan Wu¹ and Zhimin Chen⁴ 

¹ School of Information Science and Engineering, Southeast University, Nanjing 210096, China; shengshuran@seu.edu.cn (S.S.); wuln@seu.edu.cn (L.W.)

² Shannxi Key Laboratory of Integrated and Intelligent Navigation, Xi'an 710068, China; yaoyuxuan20@outlook.com

³ Xi'an Research Institute of Navigation Technology, Xi'an 710068, China

⁴ School of Electronic and Information, Shanghai Dianji University, Shanghai 201306, China; chenzm@sdju.edu.cn

* Correspondence: chenpengseu@seu.edu.cn; Tel.: +86-15895952189

Abstract: In the direction of arrival (DOA) estimation problem, when a low-bit analog to digital converter (ADC) is used, the estimation performance severely deteriorates. In this paper, the DOA estimation problem is considered in a low-cost direction finding system with low-bit ADC. To eliminate quantization noise, we propose a novel network ADCnet, which is a composition of fully connected layers and exponential linear unit (ELU) layers, and the input signals are the received signals using low-bit ADC. After the ADCnet, an AtomicNet is also proposed to estimate the DOA from the denoised signals, where atomic vectors are corresponding to the steer vectors. A loss function considering both the reconstruction performance and the sparsity is proposed in the AtomicNet. Different from the exiting atomic norm-based methods, the proposed method can avoid an optimization problem and estimate the DOA with lower computational complexity. Simulation results show that the proposed method outperforms the existing methods in the DOA estimation performance using low-bit ADC.

Keywords: DOA estimation; atomic network; low-bit ADC; sparse reconstruction



Citation: Sheng, S.; Chen, P.; Yao, Y.; Wu, L.; Chen, Z. Atomic Network-Based DOA Estimation Using Low-Bit ADC. *Electronics* **2021**, *10*, 738. <https://doi.org/10.3390/electronics10060738>

Academic Editor: Alessandro Cidronali

Received: 12 February 2021

Accepted: 17 March 2021

Published: 20 March 2021

Publisher's Note: MDPI stays neutral with regard to jurisdictional claims in published maps and institutional affiliations.



Copyright: © 2021 by the authors. Licensee MDPI, Basel, Switzerland. This article is an open access article distributed under the terms and conditions of the Creative Commons Attribution (CC BY) license (<https://creativecommons.org/licenses/by/4.0/>).

1. Introduction

The direction of arrival (DOA) [1–3] estimation problem is a fundamental problem in the application of wireless communications and radar systems [1,3–5], and an array is adopted to estimate the DOA from the different phases of the received signals. Usually, discrete Fourier transform (DFT)-based methods [6–8] can be used to estimate the DOA, where the phase difference of the received signals between different antennas can be described as spatial sampling of the signal, and the DOA estimation problem is similar to the frequency estimation problem in the time-frequency domain [9,10].

The frequency estimation performance is limited by the number of samples in the time domain [11–14], and the DOA estimation performance of the DFT-based methods is also limited when the number of antennas is fixed. The limited performance is usually called Rayleigh criterion [15,16]. The super-resolution methods are proposed to overcome the Rayleigh criterion. The most famous method is the multiple signal classification (MUSIC) method [17] and the estimating signal parameters via rotational invariance techniques (ESPRIT) method [18]. The MUSIC-based methods, including the G-MUSIC method [19], Root-MUSIC method [20] and space-time MUSIC method [21], are also proposed. Additionally, for a multichannel phased array radar, a maximum likelihood estimation with a constrained fractional quadratic optimization problem is proposed in [22] and solved by the Dinkelbach's algorithm. The sparse learning via iterative minimization (SLIM) is proposed in [23], and a better performance is obtained than the CoSaMP approach. Additionally, for the block-sparsity reconstruction, the two-dimensional (2D) spectrum sensing is addressed in [24] using a cognitive radar.

The performance improvement achieved by the MUSIC-based method is based on the subspace decomposition using the second-order statistics, such as the covariance matrix of the received signals. However, to estimate the second-order statistics exactly, many more samples must be used, so the DOA cannot be estimated in real-time. To solve this problem and also improve the DOA estimation performance, sparse-based methods have been proposed. For example, the compressed sensing (CS)-based methods [25–27] can estimate the DOA with much fewer samples. In the CS-based methods, the received signals are sparse in the spatial domain [28,29]. For example, in the multiple-input and multiple-output (MIMO) radar, a CS-based method is proposed in [28,30,31].

In the CS-based method, a type of method based on the atomic norm minimization (ANM) [32] has been proposed in recent years [33,34]. For example, joint estimation of direction-of-departure (DOD) and DOA for MIMO radar is given via two-dimensional ANM in [35,36]. W. Tang et al. considers the coprime array and presents an interpolation algorithm based on the ANM to estimate the DOA [37]. The gridless sparse signal recovery problem in the spherical harmonic domain with ANM is proposed in [38]. In the ANM-based methods, the spatial domain is described by the atomic set, and we try to find the minimal projection of the received signals in the atomic set. Then, the corresponding ANM is formulated, but it is difficult to solve the ANM problem. A semi-definite programming (SDP) method is proposed to solve the ANM problem [9,39–41].

ANM-based methods for the DOA estimation have been proposed. For example, in [42], a bi-orthogonal sparse linear array (BSLA) structure is exploited in a separable gridless DOA estimation algorithm (2D-SGFRI). A sparse nested array with coprime displacement (SNACD) is considered, and a DFC with an offset compensation (DFT-OC) method is proposed in [43]. The unknown mutual coupling is considered, and an extended signal vector is generated for the DOA estimation in [44]. T. Chen et al. exploits the vectorized covariance data of the received signals and proposes an ANM model based on complete vectorized covariance data [45]. P. Chen et al. considers the gain-phase errors and proposed a new type of atomic norm for the DOA estimation [46]. A better DOA estimation performance is achieved for the wideband DOA estimators in [47] using the atomic norm. A gridless one-bit DOA estimation approach with one-snapshot is proposed in [48] to be robust against the off-grid errors [9], but the quantization noise is not considered. However, the computational complexity of the ANM-based methods is high and cannot be solved efficiently.

Moreover, in the ANM-based methods, an infinite precision analog to digital converter (ADC) is adopted, where only the additive white Gaussian noise instead of the quantization is considered. The quantization noise is not considered in the ANM-based methods. As we all know, the DOA estimation is realized in the array with multiple antennas and radio frequency (RF) channels, and signals in each channel are sampled by ADC, so many ADC must be used in the DOA estimation problem. For a low-cost system, only low-bit ADC can be used, so the existing ANM-based methods cannot be used directly. Furthermore, the atomic set cannot be formulated easily with the quantization noise [39,49,50].

In this paper, the DOA estimation problem is considered in the scenario with low-bit ADC, which can be used in the low-price radar or wireless communication systems, since the price of the high-bit ADC is expensive and cannot be used widely. Different from the existing methods trying to describe the quantization noise exactly, the data-driven method is proposed. First, an ADCnet is proposed to denoise the signals sampled by low-bit ADC, where the output layer of ADCnet is the denoised signal. Then, an AtomicNet is proposed, with the output layer being the atomic vector. In the AtomicNet, the sparsity of the received signals in the spatial domain is exploited, so a new type of loss function composed of both reconstruction performance and sparsity is proposed. By training the AtomicNet with both an infinite precision ADC and the low-bit ADC, the better atomic vector is reconstructed. Finally, the corresponding simulation results are given using the proposed networks.

The remainder of this paper is organized as follows. The system model using low-bit ADC is described in Section 2. Then, the ADCnet for the denoise and AtomicNet for

the DOA estimation are proposed in Section 3. The simulation results are carried out in Section 4, and Section 5 finally concludes the paper.

2. System Model Using Low-Bit ADC

We consider the DOA estimation problem in the scenario using low-bit ADC, as shown in Figure 1. In the uniform linear array (ULA) with N antennas, the distance between the adjacent antennas is $\lambda/2$, where λ is the wavelength of the received signal. K far-field narrow-band signals are received by the array, so, in the n -th ($n = 0, 1, \dots, N - 1$) antenna, the received signal can be expressed as

$$y_n(t) = \mathcal{R} \left\{ \sum_{k=0}^{K-1} s_k(t) e^{j2\pi f_I t} e^{j2\pi \frac{nd}{\lambda} \sin \theta_k} \right\} + w_n(t), \quad (1)$$

where f_I is the intermediate frequency (IF), the k -th signal is denoted as $s_k(t)$, the DOA of the k -th signal is denoted as θ_k , and $w_n(t)$ is the additive white Gaussian noise in the n -th antenna.

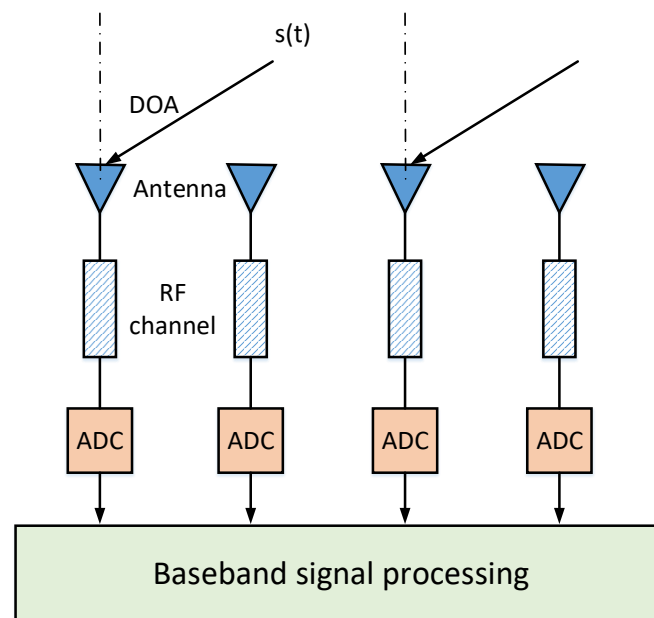


Figure 1. The system model of direction of arrival (DOA) estimation using low-bit ADC.

In the low-cost devices, the low-bit ADC is used, so the dynamics are limited in these devices. In this paper, we try to extend the ability of low-bit ADC, which means that the DOA estimation performance will be improved using the same ADC. When the low-bit ADC is adopted, we define a function $g(\cdot)$ as a signal passing the ADC. Then, the received signal passing the low-bit ADC is

$$y'_n(t) \triangleq g(y_n(t)). \quad (2)$$

The equivalent baseband representation of the received signal is

$$r_n(t) \triangleq F[y'_n(t) e^{-j2\pi f_I t}], \quad (3)$$

where $F(\cdot)$ is a low-pass filter. In the paper, we will estimate the DOA θ_k from the low-bit signal $r_n(t)$. When the low-bit ADC is used in the system, the dynamics of the received signals are narrow, since the numbers between the largest value and the smallest value in low-bit ADC are limited. Therefore, for the dynamic concern, both AGC (automatic gain control) and STC (sensitivity time control) can be used to extend the dynamic range

for low-bit ADC. The AGC technology is used to control the received signal and keep the power at the same level. The STC technology is swept-gain control and can attenuate the very strong signals returned from nearby targets in the radar receiver, so the received power can be controlled by the time. Both technologies can be used to keep the power of the received signals at the same level. Then, the low-bit ADC can be used in the scenario with a relatively large range of the received power.

Moreover, as shown in Figure 2, we define the quantization function $g(\cdot)$ as

$$g(x) = \begin{cases} V_{Q-1}, & x \geq V_{Q-1} - \frac{\Delta}{2} \\ V_q, & x \in \left[V_q - \frac{\Delta}{2}, V_q + \frac{\Delta}{2}\right), \\ V_0, & x < V_0 + \frac{\Delta}{2} \end{cases} \quad (4)$$

where Q is the number of quantization steps, Δ is the quantization step, and V_q denotes the q -th quantization value. To reconstruct the original signal from the quantized one, we can use the base idea of “multiple sampling”, where the “multiple sampling” is realized by spatial sampling using the multiple antennas.

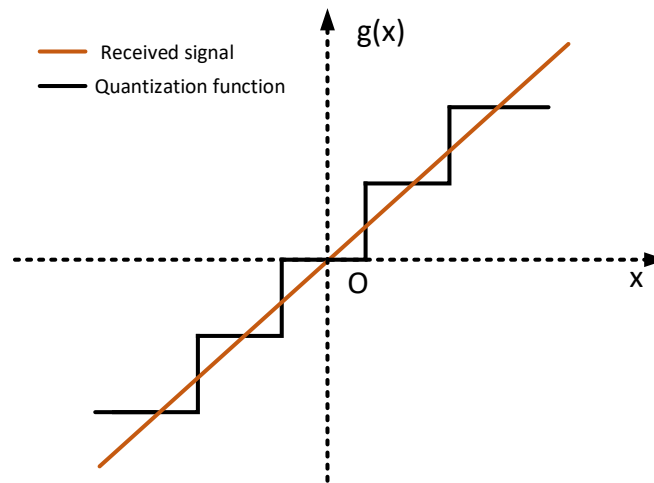


Figure 2. The quantization function.

3. The Atomic Network-Based DOA Estimation Using Low-Bit ADC

3.1. The Deep Learning-Based Quantization Denoising

Considering the signal is received by N antennas, after the low-bit ADC, the received signals are expressed in (3). We can find that multiple antennas receive the same signals with only different delays, i.e., signal phases and the additive white Gaussian noise. Then, the received signals are quantized by the low-bit ADC. We can try to exploit the relationship among the quantized signals to eliminate the quantization noise. Therefore, we propose a deep learning-based denoising method.

The model architecture is shown in Figure 3, and this deep learning network is named as ADCnet. This network is for denoising the received signals, which is sampled by a low-bit ADC and the additional quantization noise is introduced. Since the received signals are complex in the DOA estimation application, we use a vector containing the real and imaginary parts as the input quantized signal, and it is expressed as

$$\mathbf{x} = [\mathcal{R}\{r_0\}, \dots, \mathcal{R}\{r_{N-1}\}, \mathcal{I}\{r_0\}, \dots, \mathcal{I}\{r_{N-1}\}]^T. \quad (5)$$

In Figure 3, the number of antennas N is 10, so the entries in the input layer are 20 with both the real and imaginary parts. After the input layer, there are five fully connected

layers, and four exponential linear unit (ELU) layers. As shown in Figure 4, the ELU activation function is defined as

$$f_{\text{ELU}} = \begin{cases} x, & x \geq 0 \\ e^x - 1, & x < 0 \end{cases} \quad (6)$$

The ADCnet is for eliminating the quantization noise introduced by the low-bit ADC, so the loss function is defined as

$$f_{\text{Loss}} = \|\mathbf{z} - \mathbf{x}\|_2^2, \quad (7)$$

where \mathbf{z} is the output vector. In the training stage, the output signal of the ADCnet is chosen as the one without the quantization noise.

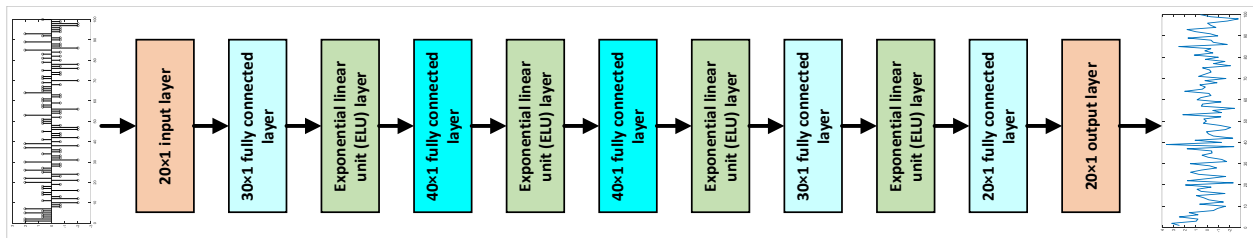


Figure 3. The model architecture for the signal reconstruction using low-bit ADC.

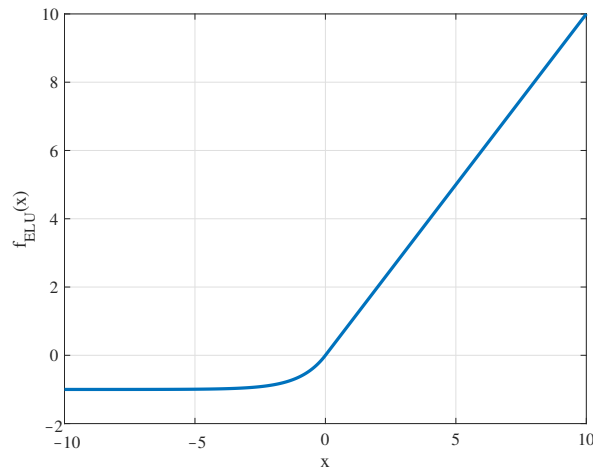


Figure 4. The exponential linear unit (ELU) activation function.

3.2. The Atomic Norm-Based DOA Estimation

After the ADCnet, the atomic norm-based method is proposed for the DOA estimation. In the DOA estimation problem, the received signals are sparse in the spatial domain. The sparsity can be measured as an atomic norm, which is defined as

$$f_{\text{atomic},0}(\mathbf{x}) \triangleq \inf \left\{ M : \mathbf{x} = \sum_{m=0}^{M-1} b_m \mathbf{a}(\theta_m) \right\}, \quad (8)$$

where we have $\theta_m \in [0, 2\pi)$, b_m is the decomposition coefficient, and we defined $\mathbf{a}(\theta)$ as the steering vector of the array. We have

$$\mathbf{a}(\theta) \triangleq \left[1, e^{j2\pi \frac{ud}{\lambda} \sin \theta}, \dots, e^{j2\pi \frac{(N-1)d}{\lambda} \sin \theta} \right]^T, \quad (9)$$

where the DOA is denoted as θ , the distance between adjacent antennas is d , and the wavelength is denoted as λ . Therefore, the atomic norm is used to show the minimum number of decompositions M in the space of steer vectors.

However, in the practical applications, the minimum number of decompositions M cannot be obtained easily. Therefore, we try to approximate the atomic norm as

$$f_{\text{atomic},0}(\mathbf{x}) \approx f_{\text{atomic}}(\mathbf{x}) \triangleq \inf \left\{ \sum_{m=0}^{M-1} |b_m| : \mathbf{x} = \sum_{m=0}^{M-1} b_m \mathbf{a}(\theta_m) \right\}. \quad (10)$$

Hence, the DOA estimation problem in the scenario with low-bit ADC can be expressed as an optimization problem

$$\begin{aligned} \min \quad & f_{\text{atomic}}(\mathbf{x}) \\ \text{s.t.} \quad & \|\mathbf{x} - \mathbf{r}\|_2^2 \leq \epsilon, \end{aligned} \quad (11)$$

where $\mathbf{r} \triangleq [r_0(t), r_1(t), \dots, r_{N-1}(t)]^T$, and $r_n(t)$ is the received signal with low-bit ADC and is defined in (3). ϵ is a parameter to control the reconstruction error, and can be determined by the system noise and the quantization noise. In the optimization problem (11), we try to find a vector \mathbf{x} to approximate the received vector \mathbf{r} sampled by the low-bit ADC, where the vector \mathbf{x} must be sparse and the sparsity is measured by the atomic norm function $f_{\text{atomic}}(\mathbf{x})$.

3.2.1. Prevision Work

To solve the optimization problem (11), the atomic norm minimization (ANM)-based methods have been proposed. When the received signals \mathbf{r} is quantized by an infinite precision, ADC and only the addition white Gaussian noise (AWGN) is considered, the ANM method can be formulated as

$$\min_{\mathbf{x}} \quad \frac{1}{2} \|\mathbf{r} - \mathbf{x}\|_2^2 + \tau f_{\text{atomic}}(\mathbf{x}), \quad (12)$$

where τ is a parameter to control the reconstruction error and is determined by the variance of noise. To solve the ANM problem (12), we obtain the corresponding Lagrangian function with the Lagrangian parameter \mathbf{u} as

$$\mathcal{L}(\mathbf{x}, \mathbf{z}, \mathbf{u}) \triangleq \frac{1}{2} \|\mathbf{r} - \mathbf{z}\|_2^2 + \tau f_{\text{atomic}}(\mathbf{x}) + \langle \mathbf{z} - \mathbf{x}, \mathbf{u} \rangle, \quad (13)$$

where we define the inner product operation as $\langle \mathbf{a}, \mathbf{b} \rangle \triangleq \mathcal{R}\{\mathbf{b}^H \mathbf{a}\}$, and $\mathcal{R}\{\cdot\}$ is used to get the real part of a complex value. Therefore, the ANM problem can be transformed into a dual problem

$$\max_{\mathbf{u}} \min_{\mathbf{x}, \mathbf{z}} \mathcal{L}(\mathbf{x}, \mathbf{z}, \mathbf{u}). \quad (14)$$

With the definition of the dual norm, the optimization problem in (14) can be simplified as

$$\begin{aligned} \max_{\mathbf{u}} \quad & \frac{1}{2} \left(\|\mathbf{r}\|_2^2 - \|\mathbf{r} - \mathbf{u}\|_2^2 \right) \\ \text{s.t.} \quad & f_{\text{atomic}}^*(\mathbf{u}) \leq \tau. \end{aligned} \quad (15)$$

$f_{\text{atomic}}^*(\mathbf{u})$ is defined as the dual norm of the atomic norm, and is expressed as

$$f_{\text{atomic}}^*(\mathbf{u}) \triangleq \sup_{\mathbf{v} \in \mathcal{A}} \langle \mathbf{v}, \mathbf{u} \rangle, \quad (16)$$

where \mathcal{A} is the atomic set and also a set of steering vectors.

Finally, a SDP is formulated to solve the dual optimization problem (15) as

$$\begin{aligned} \max_{\mathbf{u}, \mathbf{B}} \quad & \frac{1}{2} \left(\|\mathbf{r}\|_2^2 - \|\mathbf{r} - \mathbf{u}\|_2^2 \right) \\ \text{s.t.} \quad & \begin{bmatrix} \mathbf{B} & \mathbf{u} \\ \mathbf{u}^H & \tau^2 \end{bmatrix} \succeq 0 \\ & \sum_n B_{n,n+k} = \begin{cases} 1, & k = 0 \\ 0, & k \neq 0 \text{ and } -n \leq k \leq N-1-n \end{cases} \\ & \mathbf{B} \text{ is Hermitan.} \end{aligned} \quad (17)$$

The correspond DOA can be obtained by solving the SDP problem (17).

When the ANM method is used to estimate the DOA of the received signals, the estimation results are given in Figure 5, where the number of receiving antennas is 10, and the signal-to-noise ratio (SNR) of the received signal is 15 dB. In the scenario without the effect of low-bit ADC, the polynomial value can exactly show the peaks in the direction of the received signal, as shown in the dotted line of Figure 5. However, when we use a 2-bit ADC to quantize the received signal and use the ANM method to estimate the DOA, the polynomial values are shown as a red curve in Figure 5. There are more peak values with the quantized signal, and it indicates the false alarm in DOA estimation. Therefore, in the scenario with low-bit ADC, the existing work about the ANM methods cannot be used directly.

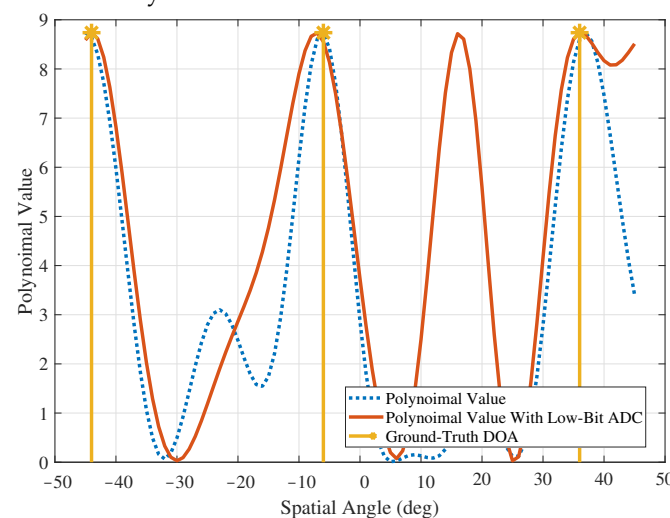


Figure 5. The DOA estimation results using the atomic norm minimization (ANM) method.

3.2.2. Proposed Atomic Network

Since the ANM-based method cannot be used in the DOA estimation problem with low-bit ADC, we propose an atomic network (AtomicNet), which can be used for the DOA estimation for the sparse and quantized signals. The architecture of the AtomicNet is shown in Figure 6, where the input of the AtomicNet is the denoised signal after the ADCnet and has both real and imaginary parts. The output of the AtomicNet is a vector corresponding to the coefficients of the atomic decomposition, and is denoted as \mathbf{c} . Hence, the reconstruction signal from the AtomicNet can be expressed as

$$\mathbf{r}_{\text{AtomicNet}} = \sum_{m=0}^{M-1} (c_m + jc_{M+m}) \mathbf{a}(\theta_m), \quad (18)$$

where c_m denotes the m -th entry of the output vector \mathbf{c} . Note that the output vector contains both the real and imaginary parts of the complex values.

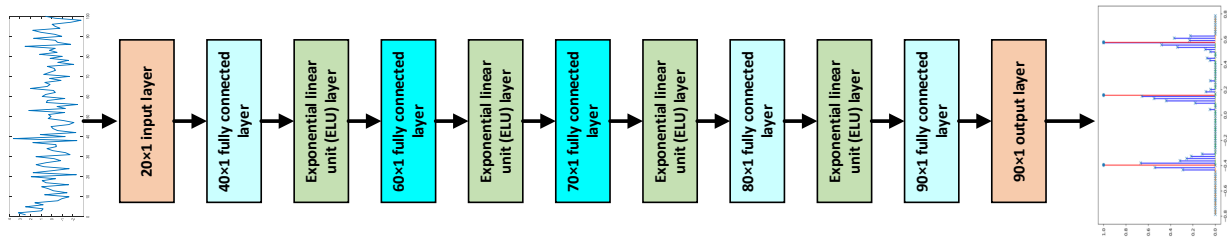


Figure 6. The model architecture for the atomic network.

In the AtomicNet, we try to reconstruct the received signal with low-bit ADC, and also consider the sparsity of the received signal in the spatial domain. Therefore, we propose a new loss function for the atomic reconstruct, and the loss function is defined as

$$f_{\text{loss}} \triangleq \frac{1}{M} \|\mathbf{r}_{\text{AtomicNet}} - \mathbf{r}_{\text{ADCnet}}\|_2^2 + \frac{\zeta}{M} \|\mathbf{c}\|_1, \quad (19)$$

where $\mathbf{r}_{\text{AtomicNet}}$ is defined in (18), and the part $\frac{1}{M} \|\mathbf{r}_{\text{AtomicNet}} - \mathbf{r}_{\text{ADCnet}}\|_2^2$ is used to control the reconstruction performance, so that the reconstruction signal can approach the received signal using low-bit ADC. The part $\|\mathbf{c}\|_1$ is the ℓ_1 norm of the AtomicNet output \mathbf{c} , and the ℓ_1 norm is used to control the sparsity of the AtomicNet output. The parameter ζ is for the trade-off between the reconstruction performance and the sparsity of the output signal.

To train the AtomicNet, we use two types of data sets. In the first data set, the input data are the received signal with the infinite precision ADC, and only the additive white Gaussian noise is considered. The input data set is generated by the array system model with different SNRs. In the second data set, the input data are the one with low-bit ADC and the additive white Gaussian noise. The reason we use two types of data sets is that, when only the low-bit ADC data set is used, and the input data are so “non-ideal,” the AtomicNet cannot be trained easily and converge to an optimal position. Therefore, we use a “good” data with an infinite precision ADC to train the AtomicNet at the first step. Then, we polish the AtomicNet using the low-bit data set at the second step.

After training the AtomicNet, we connect the AtomicNet after the ADCnet and finally obtain a network for the DOA estimation in the scenario with low-bit ADC. Furthermore, the proposed method has relatively lower computational complexity than the ANM-based methods since the interior point method is used to solve the SDP in ANM-based methods. The network-based method can avoid the optimization problem-solving processes.

4. Simulation Results

In this section, the simulation results using the proposed method for the DOA estimation using the low-bit ADC are given. A PC with Matlab R2019a and Python carries out the simulation result, and the PC has an Intel(R) Core(TM) i7-8750H CPU @ 2.20 GHz (Intel, San Jose, CA, USA). The sources are available online <https://drive.google.com/drive/folders/1bPZRQUi3cKuyzlOshIninQYV9cBPCYwV?usp=sharing> (accessed on 15 March 2021) and also are included as additional material of this paper.

To show the simulation results, the number of antennas is $N = 10$, the carrier frequency is $f_c = 1$ GHz, the wavelength is $\lambda = 0.3$ m, and the distance between the adjacent antennas is $\lambda/2$ in the ULA. After the mixers and filters, the received signals are sampled by the low-bit ADC at the intermediate frequency $f_I = 60$ MHz, where the number of the quantization bits in the ADC is 2 bits. The number of signals to detect is $K = 3$, and the detection range in the spatial domain is from -45° to 45° . The detection area is divided into 45 grids, i.e., $\mathbf{g} = [-45^\circ, -43^\circ, -41^\circ, \dots, 41^\circ, 43^\circ]^T$, so the spatial resolution is 2° .

First, to train the ADCnet, we generate the received signal with the additive white Gaussian noise, and the SNR of the received signal is from 20 dB to 100 dB. The training processes are shown in Figures 7 and 8. In Figure 7, we choose the learn rate as 2×10^{-2} , 5×10^{-2} , 8×10^{-2} and 5×10^{-3} , respectively. The corresponding values of the loss function

are also shown. We can find that, when the learning rate is 2×10^{-2} and 5×10^{-2} , better convergence can be achieved by the loss function, so the learning rate is 2×10^{-2} in the following simulations. In the training processes, stochastic gradient descent (SGD) is adopted to update the coefficients of the ADCnet. When the different values of the momentum parameter are used, the corresponding convergences are shown in Figure 8. We can find that, when the momentum is 0.9, the best convergence performance is achieved, so we choose the momentum as 0.9 in the following simulation.

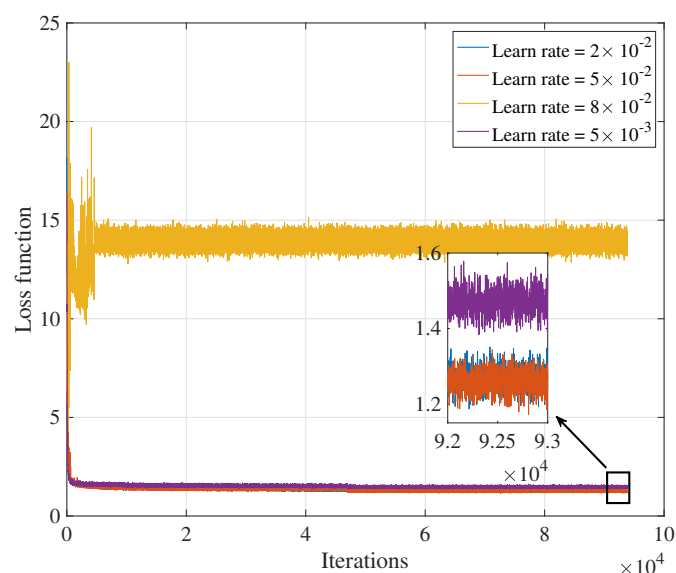


Figure 7. The loss function with different values of learning rate.

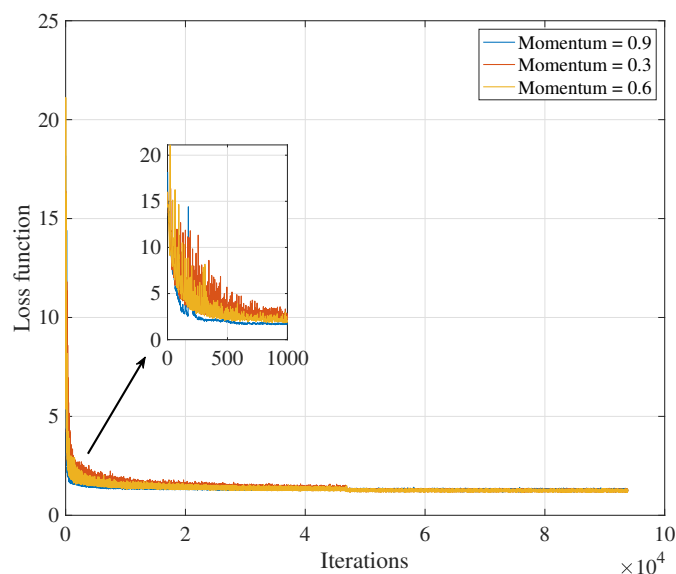


Figure 8. The loss function with different values of momentum.

Then, with the trained ADCnet, we use the 2-bit quantized signals as the input, the denoised results after the ADCnet are shown in Figure 9. We can find that the denoised signal can approach the original signal in the scenario with only 2-bit ADC. This figure shows the efficiency of the proposed ADCnet in removing the additional quantization noise.

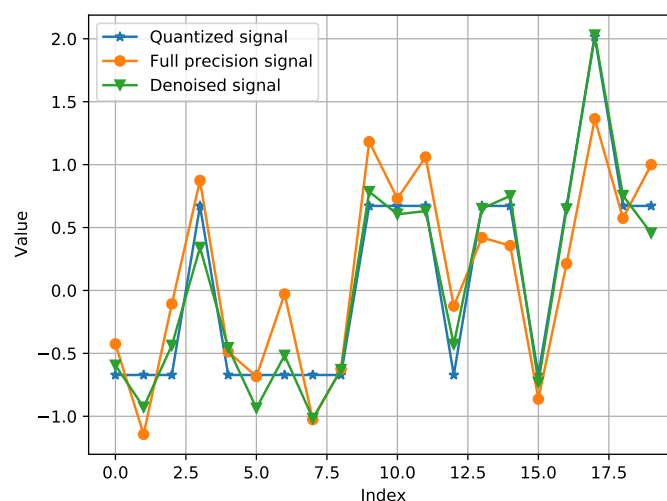


Figure 9. The denoised signals are compared with the full precision signal.

To train the AtomicNet, we use the signal with an infinite precision ADC first, and the training processes are shown in Figure 10. The values of the loss function are stable after about 10^5 episodes. The estimated sparse vector as the output of the AtomicNet is shown in Figure 11, where the DOA of the 3 signals can be estimated exactly with the DOA estimation error less than 2° .

During the second training step, we use the 2-bit quantized signals as the training data set, and the training processes are given in Figure 12. From the figure, we can find that the value of the loss function can be smaller than the one using the infinite precision ADC. The sparse reconstruction results are given in Figure 13, where the corresponding DOA of three signals are estimated exactly. This is different from the DOA estimation results in Figure 5, where the false alarm is increased as more signals are estimated.

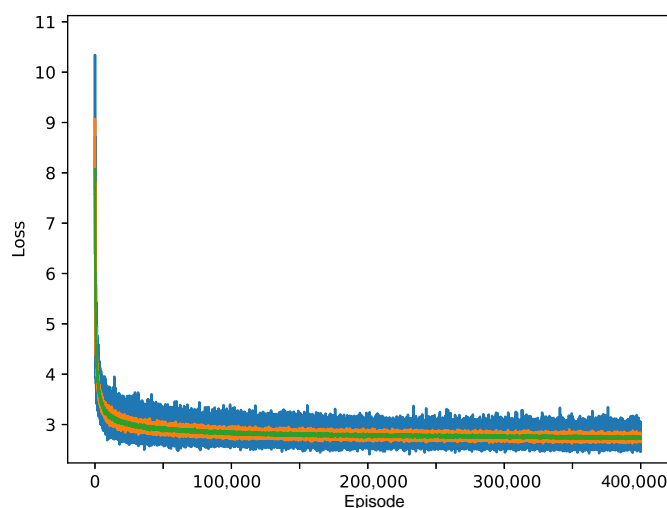


Figure 10. The loss function value in training the AtomicNet using infinite precision ADC. The blue line is the value of the loss function at each episode, the yellow line is the smoothed value with 20 episodes, and the green one is the smoothed value with 100 episodes.

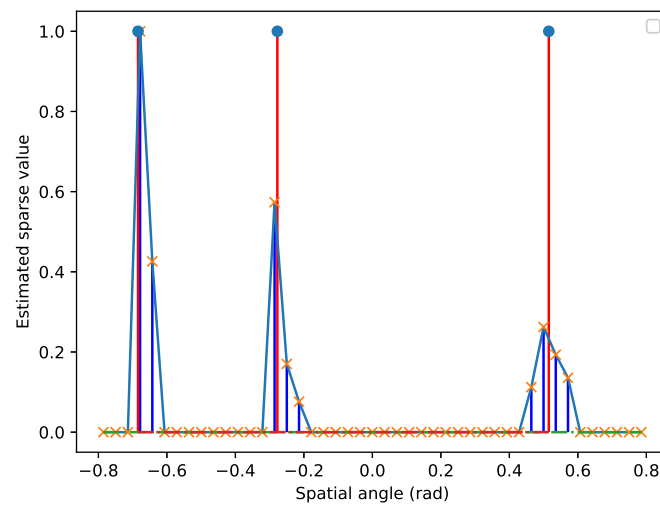


Figure 11. The reconstructed sparse signal using AtomicNet and infinite precision ADC, where the red line denotes the ground-truth DOA and the blue line denotes the estimated spatial spectrum.

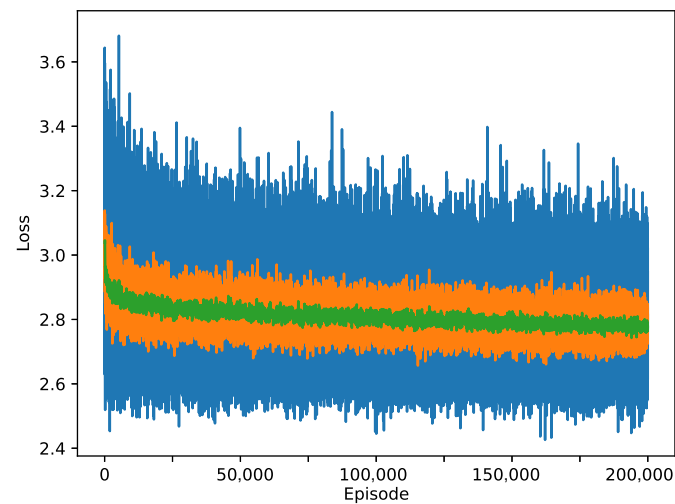


Figure 12. The loss function value in training the AtomicNet using 2-bit ADC. The blue line is the value of the loss function at each episode, the yellow line is the smoothed value with 20 episodes, and the green one is the smoothed value with 100 episodes.

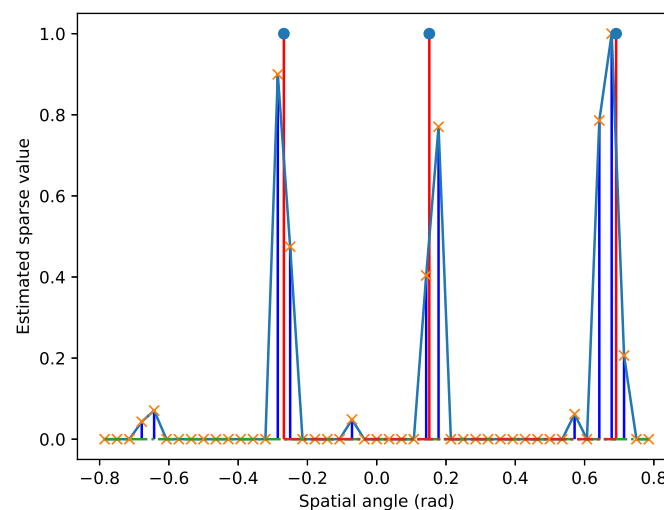


Figure 13. The reconstructed sparse signal using AtomicNet and 2-bit ADC, where the red line denotes the ground-truth DOA and the blue line denotes the estimated spatial spectrum.

In the practical systems, the power of the received signals can be different, so we try to estimate the DOA with the power being 1, 0.64, and 0.25. The estimated results are shown in Figure 14, and we can find that the DOA can be estimated successfully. Additionally, the estimated power can also approach the ground-truth power. Therefore, the proposed method can be also used in the scenario with different received power.

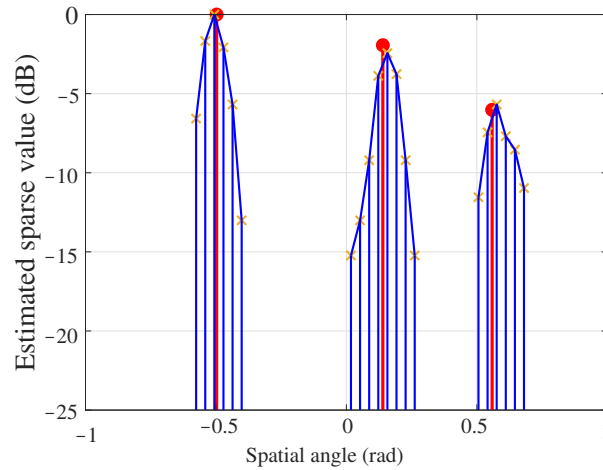


Figure 14. The reconstructed sparse signal with different power using AtomicNet and 2-bit ADC, where the red line denotes the ground-truth DOA, and the blue line denotes the estimated spatial spectrum.

Finally, the DOA estimation performance using low-bit ADC is shown, and the simulation results are given in Figures 15–17, where the 3-bit ADC, 2-bit ADC, and 1-bit ADC are used, respectively. The proposed method is compared with the existing methods: (1) Fast Fourier transformation (FFT) method, where we use the spatial FFT to estimate the DOA; (2) ANM method, where we use the existing ANM-based method to estimate the DOA. The estimation performance is measured by the root mean square error (RMSE), which is defined as

$$\text{RMSE} = \sqrt{\frac{1}{KP} \sum_{p=0}^{P-1} \sum_{k=0}^{K-1} |\hat{\theta}_{k,p} - \theta_{k,p}|^2}, \quad (20)$$

where $\theta_{k,p}$ is the DOA of the k -th signal during the p -th measurement, and $\hat{\theta}_{k,p}$ is the estimated DOA corresponding to the k -th signal during the p -th measurement.

In Figure 15, we can find that the proposed method outperforms both the FFT method and ANM method in the scenario with lower SNR (less than 5 dB). When the SNR is 0 dB, the RMSE of the DOA estimation using the FFT method, the ANM method, and the proposed method are 3.2°, 2.9°, and 2.5°, respectively. Hence, the DOA estimation performance is improved by about 16% compared to the existing ANM method with SNR being 0 dB. Similarly, when the 2-bit ADC is adopted, the corresponding DOA estimation is shown in Figure 16. The proposed method shows better estimation performance than both the FFT method and the ANM method. The RMSE is improved about 10% using the proposed method with the SNR being 0 dB.

When the 1-bit ADC is used, the DOA estimation performance is improved more significantly, as shown in Figure 17. The RMSE of the DOA estimation performance can approach about 1.9° with the SNR being 15 dB, but the RMSEs are only 2.1° and 2.3° using the ANM method and the FFT method, respectively. The estimation performance is improved by about 10.5% compared to the ANM method. Additionally, the estimation performance cannot be further improved with better SNR when the FFT method and the ANM method are used. Therefore, from the simulation results in Figures 15–17, we can find that the proposed DOAnet and AtomicNet can achieve better DOA estimation performance

in the scenario using the low-bit ADC, especially using the 1-bit ADC. In Figure 17, we can find that the RMSE using the FFT method with the SNR being 20 dB is about 2.4, which is the same as the performance using the proposed method with the SNR being 7 dB. Therefore, the estimation performance is improved by about 13 dB, which is equal to the improvement of 2.17 bits.

In the simulation results, the DOA estimation problems using 1-bit, 2-bit, and 3-bit ADC are considered, and the corresponding performance of the DOA estimation is also given. These simulation results show the proposed method is effective in improving DOA estimation performance using the same ADC. Furthermore, when a better ADC is used, such as 8-bit or 12-bit ADC, which is used in most radar applications, the DOA estimation performance can also be improved using the proposed method.

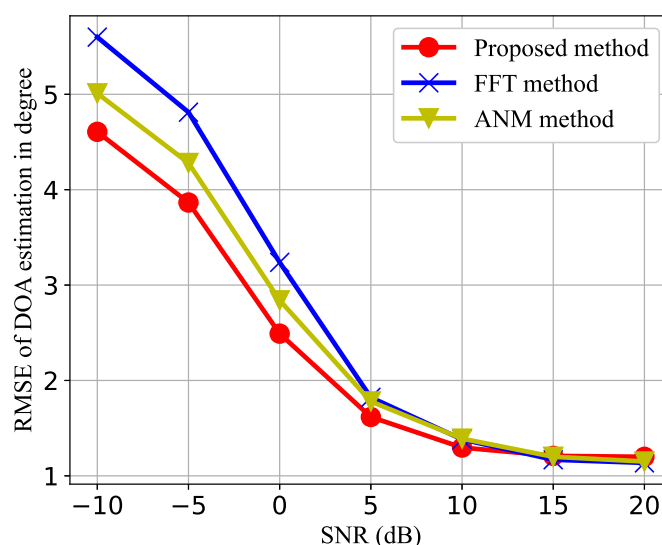


Figure 15. The root mean square error (RMSE) of the DOA estimation using 3-bit ADC to show the performance of the proposed networks.

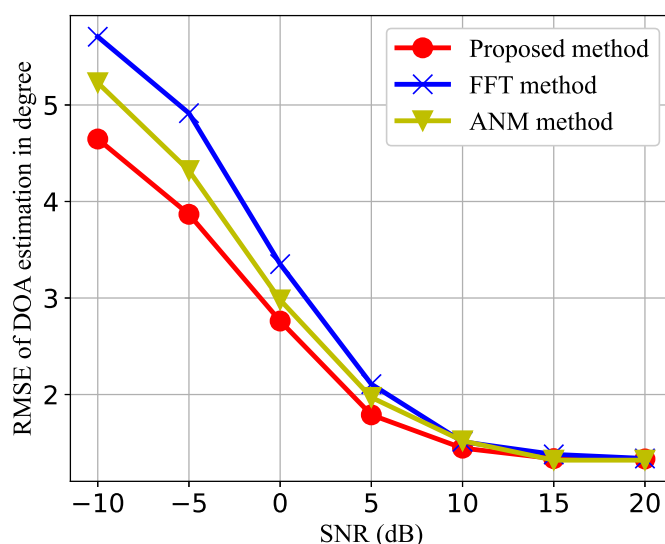


Figure 16. The RMSE of the DOA estimation using 2-bit ADC to show the performance of the proposed networks.

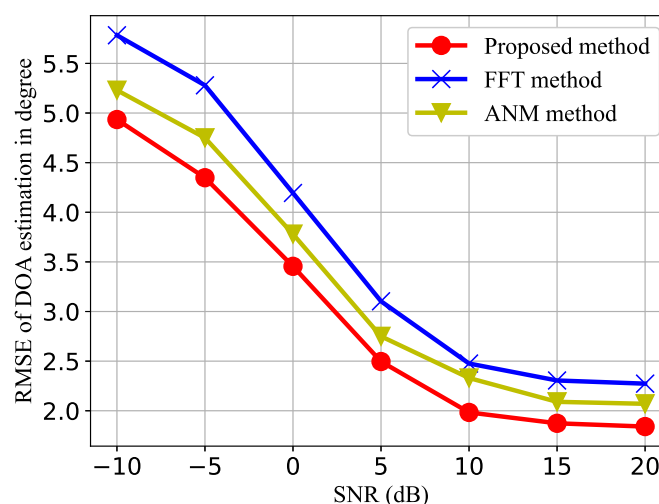


Figure 17. The RMSE of the DOA estimation using 1-bit ADC to show the performance of the proposed networks.

5. Conclusions

The DOA estimation problem in the scenario using the low-bit ADC has been considered, and we have proposed the ADCnet to denoise the received signals and the AtomicNet to estimate the DOA with the low-bit ADC. We have given the details about training the proposed networks and showed the convergence of networks. The proposed method has been compared with the existing methods such as the FFT method and the ANM method. The simulation results have shown that better estimation performance can be achieved using the proposed method, especially in the scenario with the 1-bit ADC. Further work will focus on the DOA estimation using imperfect hardware.

Author Contributions: Conceptualization, S.S. and P.C.; methodology, S.S.; software, P.C.; validation, L.W.; formal analysis, S.S.; investigation, Z.C.; resources, L.W.; data curation, S.S.; writing—original draft preparation, S.S.; writing—review and editing, S.S.; visualization, Z.C.; supervision, L.W.; project administration, Y.Y.; funding acquisition, P.C. All authors have read and agreed to the published version of the manuscript.

Funding: This work was supported in part by the foundation of Shannxi Key Laboratory of Integrated and Intelligent Navigation (Grant No. SKLIIN-20190204), the National Key R&D Program of China (Grant No. 2019YFE0120700), the National Natural Science Foundation of China (Grant No. 61801112), the Natural Science Foundation of Jiangsu Province (Grant No. BK20180357), and the Open Program of State Key Laboratory of Millimeter Waves at Southeast University (Grant No. K202029).

Conflicts of Interest: The authors declare no conflict of interest.

References

- Chen, K.T.; Ma, W.H.; Hwang, Y.T.; Chang, K.Y. A Low Complexity, High Throughput DoA Estimation Chip Design for Adaptive Beamforming. *Electronics* **2020**, *9*, 641. [\[CrossRef\]](#)
- Zhang, B.; Zou, X.; Zhang, T.; Tang, Y.; Zeng, H. A Fast Estimation Method for Direction of Arrival Using Tripole Vector Antenna. *Sensors* **2020**, *20*, 5008. [\[CrossRef\]](#) [\[PubMed\]](#)
- Liu, S.; Tang, L.; Bai, Y.; Zhang, X. A Sparse Bayesian Learning-Based DOA Estimation Method With the Kalman Filter in MIMO Radar. *Electronics* **2020**, *9*, 347. [\[CrossRef\]](#)
- Wu, X.; Zhu, W.; Yan, J. Atomic Norm Based Localization of Far-Field and Near-Field Signals with Generalized Symmetric Arrays. In Proceedings of the ICASSP 2020—2020 IEEE International Conference on Acoustics, Speech and Signal Processing (ICASSP), Barcelona, Spain, 4–8 May 2020; pp. 4762–4766.
- Kim, S.; Oh, D.; Lee, J. Joint DFT-ESPRIT estimation for TOA and DOA in vehicle FMCW radars. *IEEE Antennas Wirel. Propag. Lett.* **2015**, *14*, 1710–1713. [\[CrossRef\]](#)
- Zheng, L.; Lops, M.; Wang, X. Adaptive Interference Removal for Uncoordinated Radar/Communication Coexistence. *IEEE J. Sel. Top. Signal Process.* **2018**, *12*, 45–60. [\[CrossRef\]](#)

7. Wu, X.; Yan, J. A Second-Order Statistics-Based Mixed Sources Localization Method With Symmetric Sparse Arrays. *IEEE Commun. Lett.* **2020**, *24*, 1695–1699. [\[CrossRef\]](#)
8. Burintramart, S.; Sarkar, T.K.; Zhang, Y.; Salazar-Palma, M. Nonconventional least squares optimization for DOA estimation. *IEEE Trans. Antennas Propag.* **2007**, *55*, 707–714. [\[CrossRef\]](#)
9. Ling, Y.; Gao, H.; Ru, G.; Chen, H.; Li, B.; Cao, T. Grid Reconfiguration Method for Off-Grid DOA Estimation. *Electronics* **2019**, *8*, 1209. [\[CrossRef\]](#)
10. Liu, L.; Liu, H. Joint estimation of DOA and TDOA of multiple reflections in mobile communications. *IEEE Access* **2016**, *4*, 3815–3823. [\[CrossRef\]](#)
11. Chen, P.; Cao, Z.; Chen, Z.; Liu, L.; Feng, M. Compressed Sensing-Based DOA Estimation with Unknown Mutual Coupling Effect. *Electronics* **2018**, *7*, 424. [\[CrossRef\]](#)
12. Heckel, R.; Soltanolkotabi, M. Generalized Line Spectral Estimation via Convex Optimization. *IEEE Trans. Inf. Theory* **2018**, *64*, 4001–4023. [\[CrossRef\]](#)
13. Lu, A.; Guo, Y.; Li, N.; Yang, S. Efficient Gridless 2D Direction-of-Arrival Estimation for Coprime Array Based on Decoupled Atomic Norm Minimization. *IEEE Access* **2020**, *8*, 57786–57795. [\[CrossRef\]](#)
14. Bhaskar, B.N.; Tang, G.; Recht, B. Atomic Norm Denoising With Applications to Line Spectral Estimation. *IEEE Trans. Signal Process.* **2013**, *61*, 5987–5999. [\[CrossRef\]](#)
15. Rueckner, W.; Papaliolios, C. How to beat the Rayleigh resolution limit: A lecture demonstration. *Am. J. Phys.* **2002**, *70*, 587. [\[CrossRef\]](#)
16. Chen, P.; Cao, Z.; Chen, Z.; Yu, C. Sparse DOD/DOA Estimation in a Bistatic MIMO Radar With Mutual Coupling Effect. *Electronics* **2018**, *7*, 341. [\[CrossRef\]](#)
17. Schmidt, R.O. Multiple emitter location and signal parameter estimation. *IEEE Trans. Antennas Propag.* **1986**, *34*, 276–280. [\[CrossRef\]](#)
18. Roy, R.; Kailath, T. ESPRIT-estimation of signal parameters via rotational invariance techniques. *IEEE Trans. Acoust. Speech Signal Process.* **1989**, *37*, 984–995. [\[CrossRef\]](#)
19. Vallet, P.; Mestre, X.; Loubaton, P. Performance analysis of an improved MUSIC DoA estimator. *IEEE Trans. Signal Process.* **2015**, *63*, 6407–6422. [\[CrossRef\]](#)
20. Zoltowski, M.D.; Kautz, G.M.; Silverstein, S.D. Beam-space Root-MUSIC. *IEEE Trans. Signal Process.* **1993**, *41*, 344–364. [\[CrossRef\]](#)
21. Claudio, E.D.D.; Parisi, R.; Jacovitti, G. Space time MUSIC: Consistent signal subspace estimation for wideband sensor arrays. *IEEE Trans. Signal Process.* **2018**, *66*, 2685–2699. [\[CrossRef\]](#)
22. Aubry, A.; Maio, A.D.; Marano, S.; Rosamilia, M. Single-Pulse Simultaneous Target Detection and Angle Estimation in a Multichannel Phased Array Radar. *IEEE Trans. Signal Process.* **2020**, *68*, 6649–6664. [\[CrossRef\]](#)
23. Tan, X.; Roberts, W.; Li, J.; Stoica, P. Sparse Learning via Iterative Minimization With Application to MIMO Radar Imaging. *IEEE Trans. Signal Process.* **2010**, *59*, 1088–1101. [\[CrossRef\]](#)
24. Aubry, A.; Carotenuto, V.; De Maio, A.; Govoni, M.A. Multi-Snapshot Spectrum Sensing for Cognitive Radar via Block-Sparsity Exploitation. *IEEE Trans. Signal Process.* **2019**, *67*, 1396–1406. [\[CrossRef\]](#)
25. Yang, Z.; Xie, L. Exact joint sparse frequency recovery via optimization methods. *IEEE Trans. Signal Process.* **2016**, *64*, 5145–5157. [\[CrossRef\]](#)
26. Chen, Z.; He, X.; Cao, Z.; Jin, Y.; Li, J. Position Estimation of Automatic-Guided Vehicle Based on MIMO Antenna Array. *Electronics* **2018**, *7*, 193. [\[CrossRef\]](#)
27. Li, W.T.; Lei, Y.J.; Shi, X.W. DOA estimation of time-modulated linear array based on sparse signal recovery. *IEEE Antennas Wirel. Propag. Lett.* **2017**, *16*, 2336–2340. [\[CrossRef\]](#)
28. Yu, Y.; Petropulu, A.P.; Poor, H.V. Measurement matrix design for compressive sensing-based MIMO radar. *IEEE Trans. Signal Process.* **2011**, *59*, 5338–5352. [\[CrossRef\]](#)
29. Xiong, W.; Greco, M.; Gini, F.; Zhang, G.; Peng, Z. SFMM design in colocated CS-MIMO radar for jamming and interference joint suppression. *IET Radar Sonar Navig.* **2018**, *12*, 702–710. [\[CrossRef\]](#)
30. Chen, P.; Zheng, L.; Wang, X.; Li, H.; Wu, L. Moving target detection using colocated MIMO radar on multiple distributed moving platforms. *IEEE Trans. Signal Process.* **2017**, *65*, 4670–4683. [\[CrossRef\]](#)
31. Compaleo, J.; Gupta, I.J. Application of Sparse Representation to Bartlett Spectra for Improved Direction of Arrival Estimation. *Sensors* **2021**, *21*, 77. [\[CrossRef\]](#)
32. Chen, P.; Cao, Z.; Chen, Z.; Wang, X. Off-Grid DOA Estimation Using Sparse Bayesian Learning in MIMO Radar With Unknown Mutual Coupling. *IEEE Trans. Signal Process.* **2019**, *67*, 208–220. [\[CrossRef\]](#)
33. Chi, Y.; Da Costa, M.F. Harnessing Sparsity over the Continuum: Atomic Norm Minimization for Super Resolution. *arXiv* **2019**, arXiv:1904.04283.
34. Castro, Y.; Gamboa, F. Exact reconstruction using Beurling minimal extrapolation. *J. Math. Anal. Appl.* **2012**, *395*, 336–354. [\[CrossRef\]](#)
35. Tang, W.; Jiang, H.; Pang, S. Grid-Free DOD and DOA Estimation for MIMO Radar via Duality-Based 2D Atomic Norm Minimization. *IEEE Access* **2019**, *7*, 60827–60836. [\[CrossRef\]](#)
36. Xie, Y.; Huang, M.; Zhang, Y.; Duan, T.; Wang, C. Two-Stage Fast DOA Estimation Based on Directional Antennas in Conformal Uniform Circular Array. *Sensors* **2021**, *21*, 276. [\[CrossRef\]](#)

-
37. Tang, W.; Jiang, H.; Pang, S. Coprime Array Interpolation for Direction of Arrival Estimation Based on Atomic Norm Minimization. In Proceedings of the 2019 IEEE Radar Conference (RadarConf), Boston, MA, USA, 22–26 April 2019; pp. 1–5.
 38. Pan, J. Spherical Harmonic Atomic Norm and its Application to DOA Estimation. *IEEE Access* **2019**, *7*, 156555–156568. [[CrossRef](#)]
 39. Teke, O.; Vaidyanathan, P.P. On the role of the bounded lemma in the SDP formulation of atomic norm problems. *IEEE Signal Process. Lett.* **2017**, *24*, 972–976. [[CrossRef](#)]
 40. Chi, Y. Guaranteed Blind Sparse Spikes Deconvolution via Lifting and Convex Optimization. *IEEE J. Sel. Top. Signal Process.* **2016**, *10*, 782–794. [[CrossRef](#)]
 41. Unser, M. A unifying representer theorem for inverse problems and machine learning. *arXiv* **2019**, arXiv:math.OA/1903.00687.
 42. Wang, K.; Shi, L.; Chen, T. Two-Dimensional Separable Gridless Direction-of-Arrival Estimation Based on Finite Rate of Innovation. *IEEE Access* **2021**, *9*, 17275–17283. [[CrossRef](#)]
 43. Li, J.; He, Y.; Ma, P.; Zhang, X.; Wu, Q. Direction of Arrival Estimation Using Sparse Nested Arrays With Coprime Displacement. *IEEE Sens. J.* **2021**, *21*, 5282–5291. [[CrossRef](#)]
 44. Teng, L.; Wang, Q.; Wang, X.; Li, C. Gridless DOA Estimation Algorithm for Strictly Noncircular Sources under Unknown Mutual Coupling. In Proceedings of the 2020 IEEE International Conference on Computational Electromagnetics (ICCEM), Singapore, 24–26 August 2020; pp. 141–143.
 45. Chen, T.; Shi, L.; Guo, L. Gridless Direction of Arrival Estimation Exploiting Sparse Linear Array. *IEEE Signal Process. Lett.* **2020**, *27*, 1625–1629. [[CrossRef](#)]
 46. Chen, P.; Chen, Z.; Cao, Z.; Wang, X. A New Atomic Norm for DOA Estimation With Gain-Phase Errors. *IEEE Trans. Signal Process.* **2020**, *68*, 4293–4306. [[CrossRef](#)]
 47. Jiang, Y.; Li, D.; Wu, X.; Zhu, W. A Gridless Wideband DOA Estimation Based On Atomic Norm Minimization. In Proceedings of the 2020 IEEE 11th Sensor Array and Multichannel Signal Processing Workshop (SAM), Hangzhou, China, 8–11 June 2020; pp. 1–5.
 48. Wei, Z.; Wang, W.; Dong, F.; Liu, Q. Gridless One-Bit Direction-of-Arrival Estimation Via Atomic Norm Denoising. *IEEE Commun. Lett.* **2020**, *24*, 2177–2181. [[CrossRef](#)]
 49. Yang, Z.; Xie, L. Enhancing sparsity and resolution via reweighted atomic norm minimization. *IEEE Trans. Signal Process.* **2016**, *64*, 995–1006. [[CrossRef](#)]
 50. Wu, X.; Zhu, W.; Yan, J. A Toeplitz covariance matrix reconstruction approach for direction-of-arrival estimation. *IEEE Trans. Veh. Technol.* **2017**, *66*, 8223–8237. [[CrossRef](#)]